

Gamma-ray spectroscopy III

Andreas Görgen
DAPNIA/SPhN, CEA Saclay
F-91191 Gif-sur-Yvette
France
agoergen@cea.fr

Lectures presented at the
IoP Nuclear Physics Summer School
September 4 – 17, 2005
Chester, UK

Outline

First lecture

- Properties of γ -ray transitions
- Fusion-evaporation reactions
- Germanium detector arrays
- Coincidence technique
- Nuclear deformations
- Rotation of deformed nuclei
- Pair alignment
- Superdeformed nuclei
- Hyperdeformed nuclei
- Triaxiality and wobbling

Second lecture

- Angular distribution
- Linear polarization
- Jacobi shape transition
- Charged-particle detectors
- Neutron detectors
- Prompt proton decay
- Recoil-decay tagging
- Rotation and deformation alignment

Third lecture

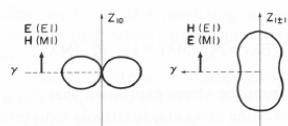
- Spectroscopy of transfermium nuclei
- Conversion-electron spectroscopy
- Quadrupole moments and transition rates
- Recoil-distance method
- Doppler shift attenuation method
- Fractional Doppler shift method
- Magnetic moments
- Perturbed angular distribution
- Magnetic Rotation
- Shears Effect

Fourth lecture

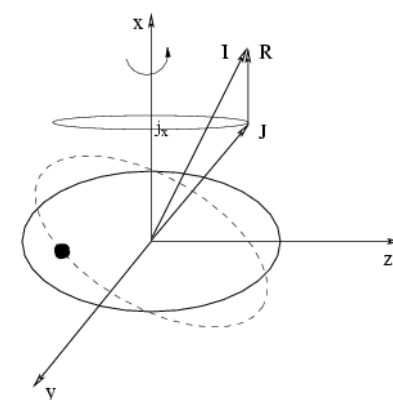
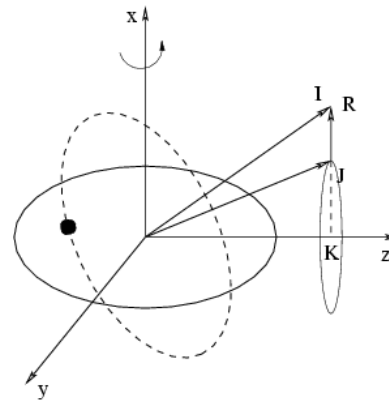
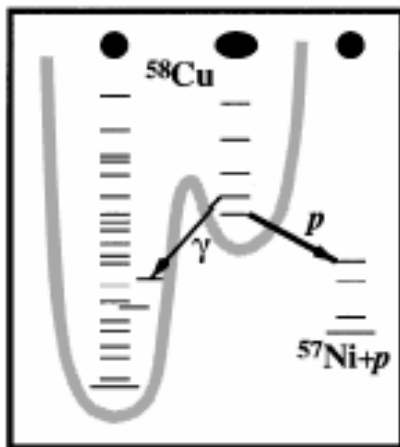
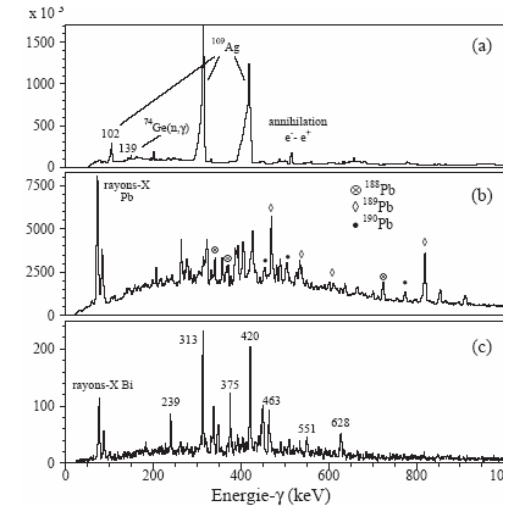
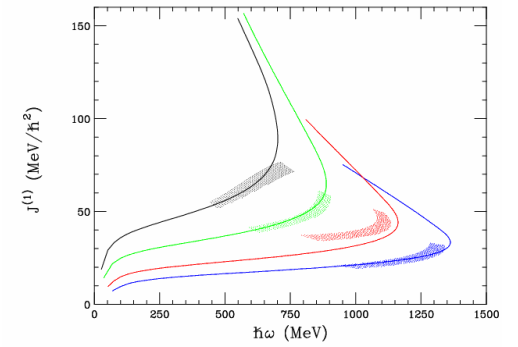
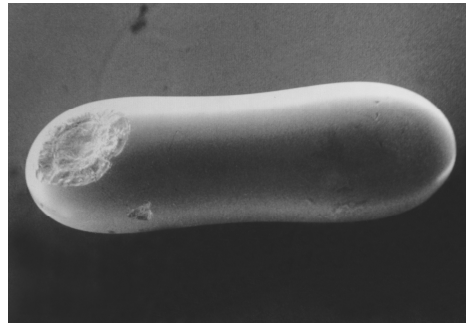
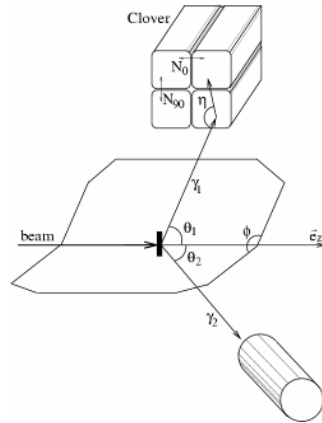
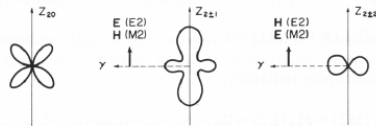
- Fast fragmentation beams
- Isomer spectroscopy after fragmentation
- E0 transitions
- Shape coexistence
- Two-level mixing
- Coulomb excitation
- Reorientation effect
- ISOL technique
- Low-energy Coulomb excitation of ^{74}Kr
- Relativistic Coulomb excitation of ^{58}Cr
- Gamma-ray tracking
- AGATA

Summary (II)

Dipol



Quadrupol

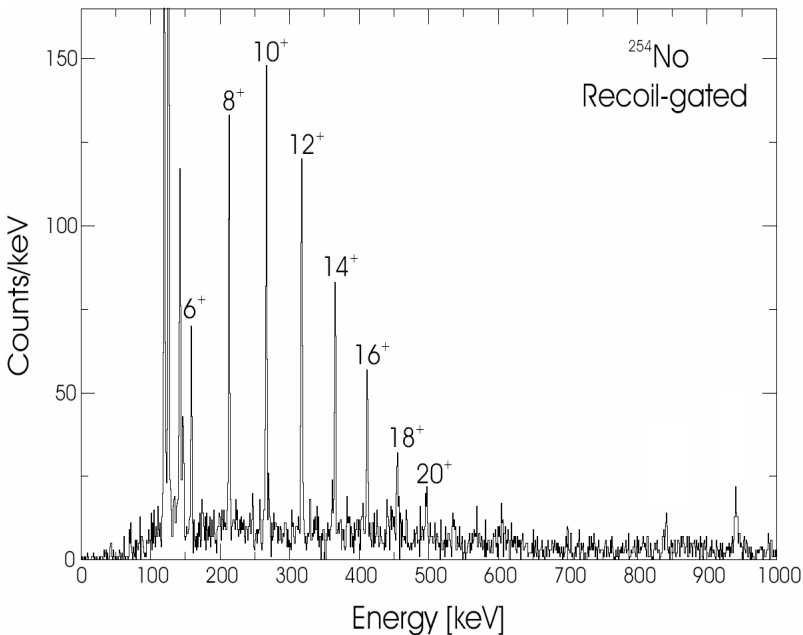


Spectroscopy of heavy elements

- Recoil-decay tagging is highly selective.
- It allows to study extremely weak structures in a huge background.
- α -decay tagging in
 - very neutron-deficient heavy nuclei
 - very heavy nuclei: Transfermia ($Z \geq 100$)
- (α emitters with tiny cross sections)

$^{109}\text{Ag}(^{83}\text{Kr},3n)^{189}\text{Bi}$
 $\sigma = 12\mu\text{b}$
 $T_{1/2} = 667\text{ ms}$

$^{208}\text{Pb}(^{48}\text{Ca},2n)^{254}\text{No}$
 $\sigma = 3.4\mu\text{b}$
 $T_{1/2} = 48\text{ s}$

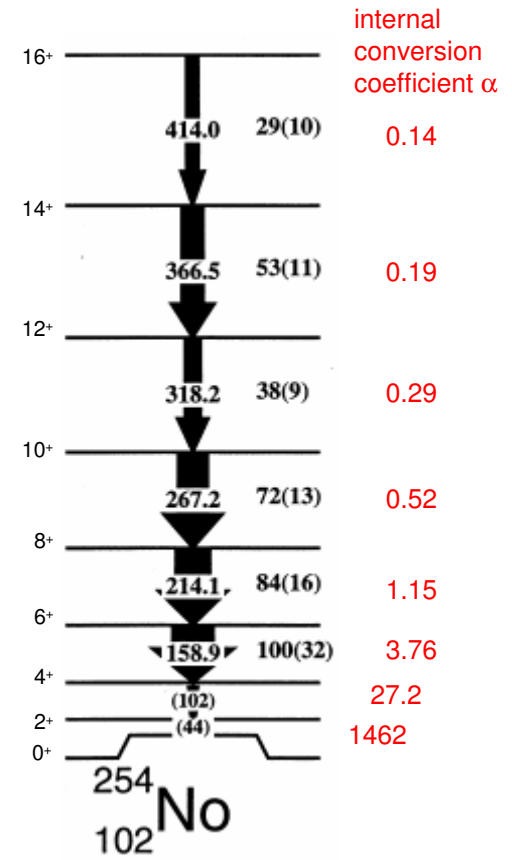


S. Eeckhaudt et al.,
 Eur. Phys. J. A, in press

Rotational band \Leftrightarrow deformation
 Compare moment of inertia $\mathcal{J}^{(2)}$
 with calculations.

We can still correlate prompt γ rays with α decay after a half life of 48 s !

strongly converted transitions
 \Rightarrow conversion-electron spectroscopy



Internal conversion

Energy difference between states carried away by atomic electron:

$$E_e = E_\gamma - B_e \quad (K, L_I, L_{II}, L_{III}, \dots)$$

B_e binding energy of the shell

Overlap of electron and nuclear wave functions, not a two-step process.

Internal conversion coefficients:

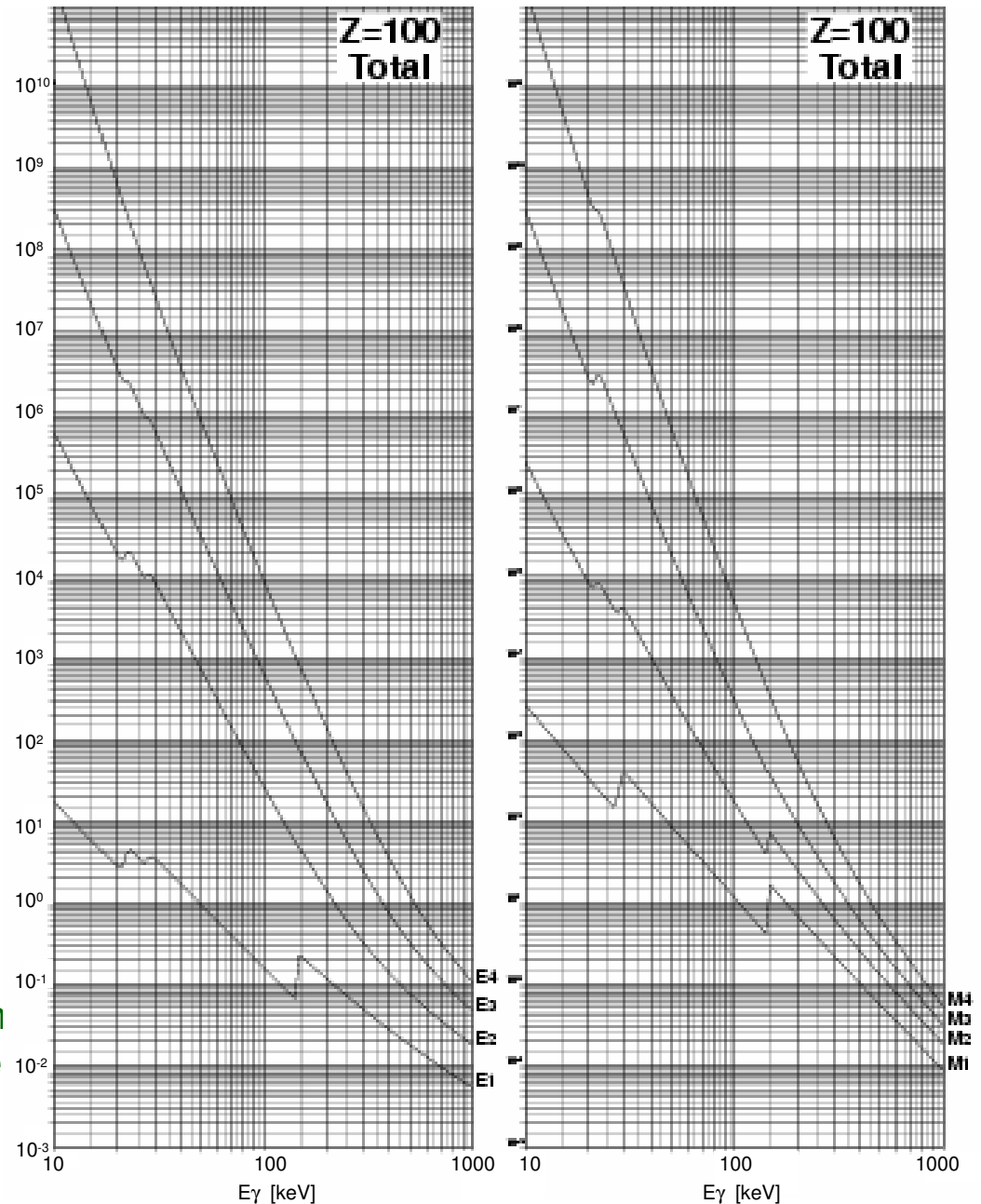
$$\alpha_{\text{tot}} = \frac{N_e}{N_\gamma} = \alpha_K + \alpha_L + \dots$$

$$N_{\text{tot}} = N_e + N_\gamma = (1 + \alpha_{\text{tot}})N_\gamma$$

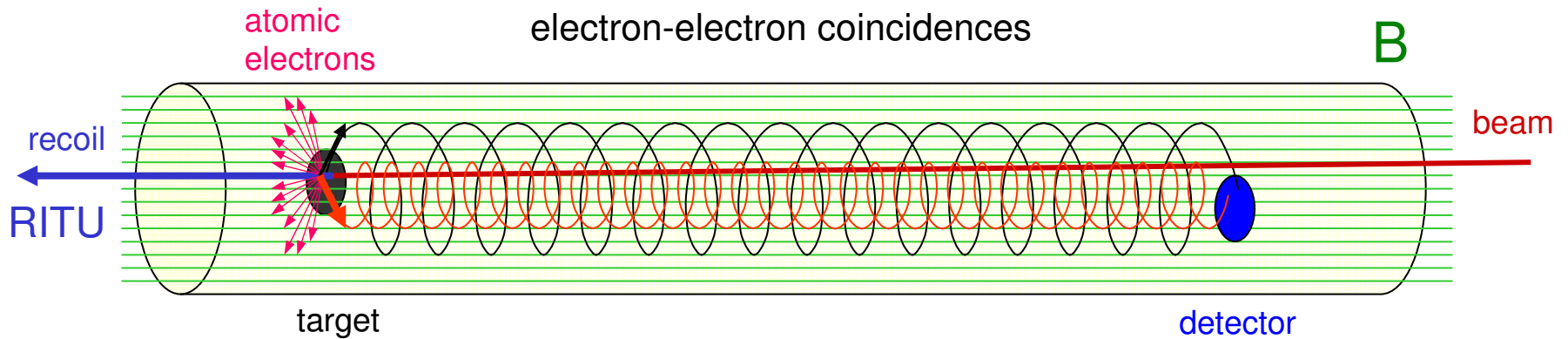
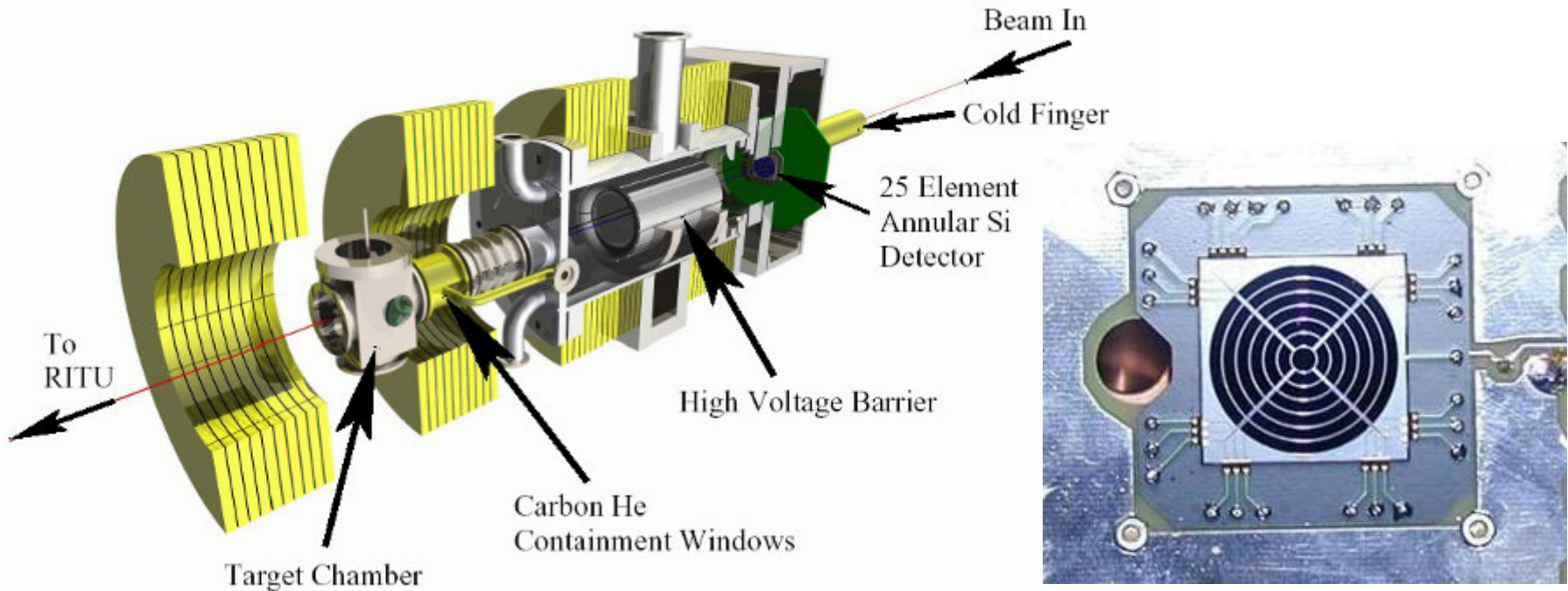
Strong dependence on

- transition energy
- multipolarity EL or ML
- atomic number Z

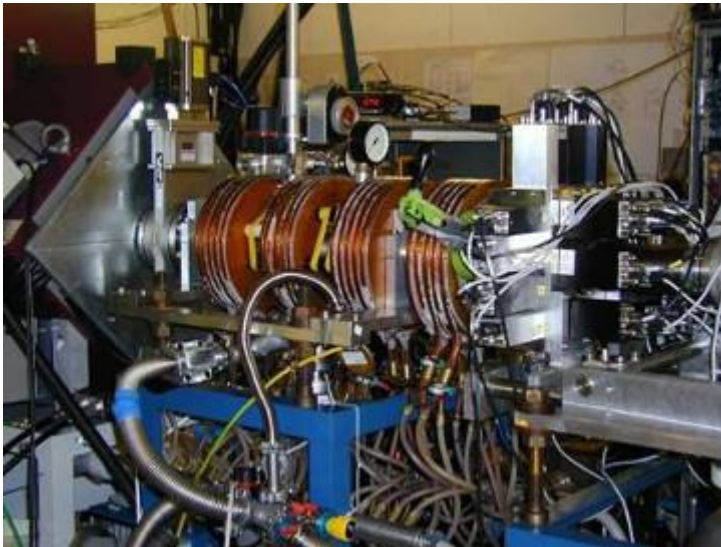
By measuring the internal conversion coefficient, it is possible to determine the multipolarity of a transition.



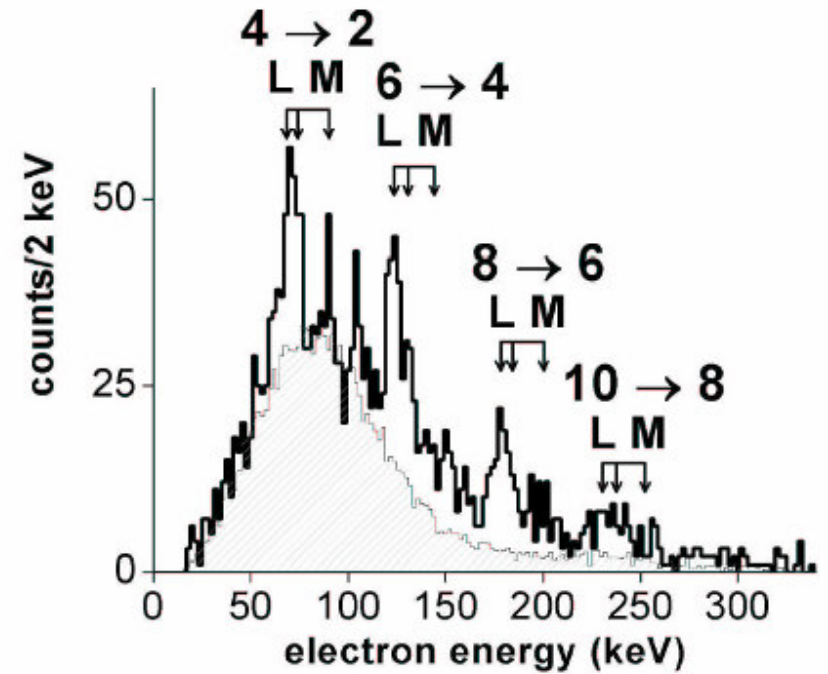
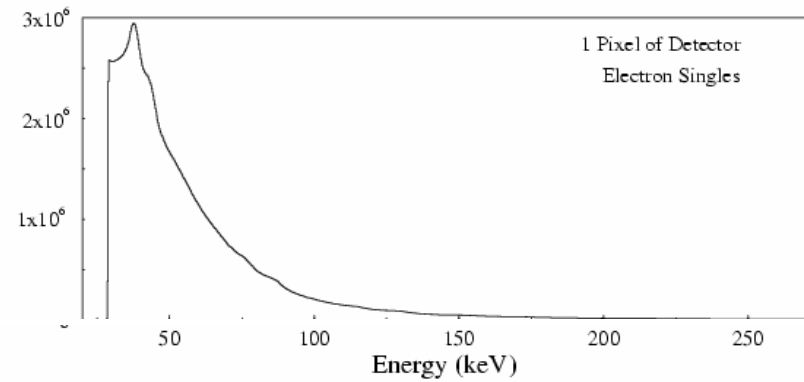
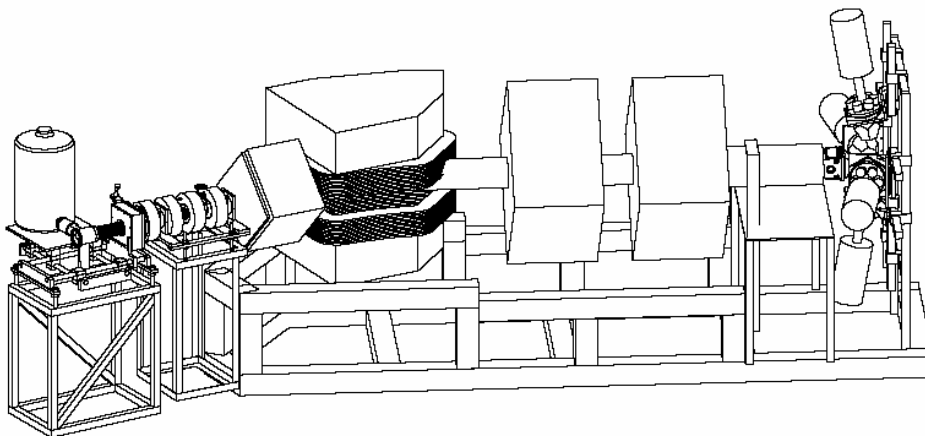
Prompt conversion-electron spectroscopy: SACRED



Prompt conversion-electron spectroscopy of ^{254}No



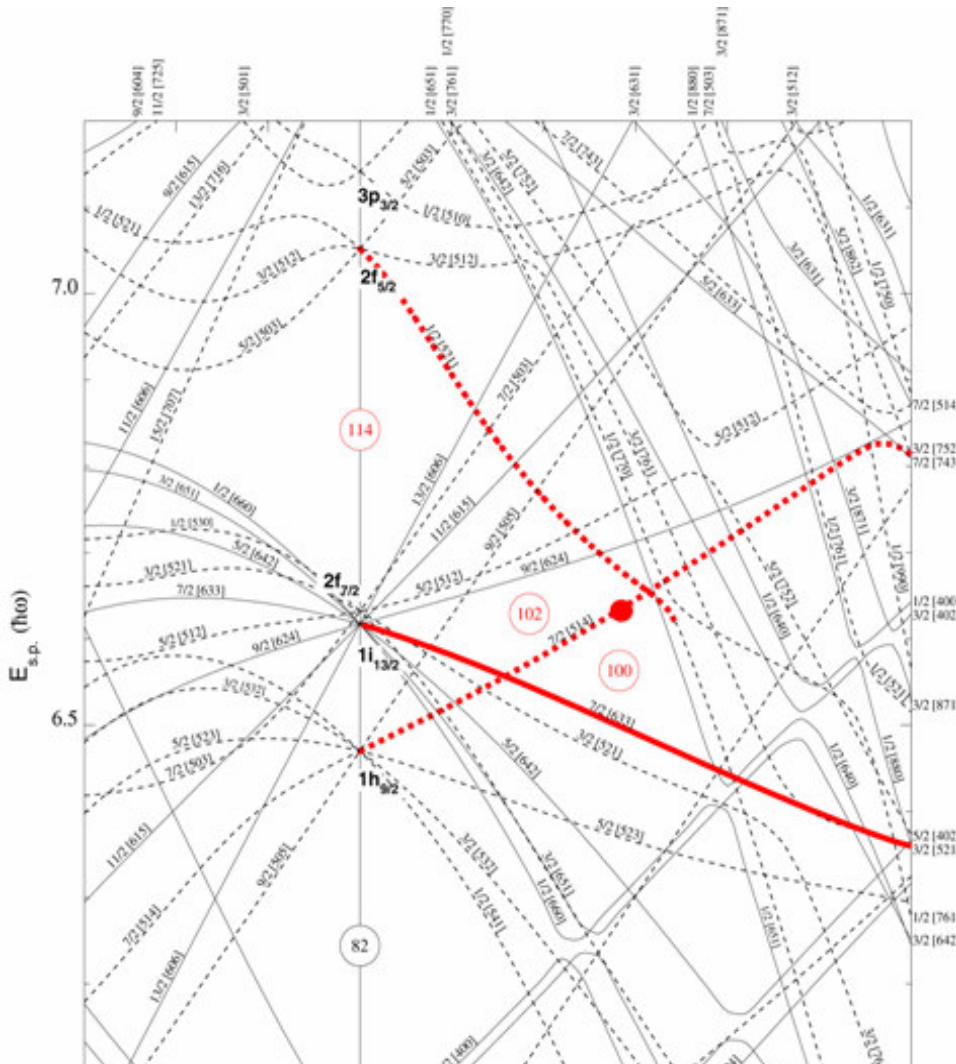
SACRED and RITU



P.A. Butler et al., Phys. Rev. Lett. 89, 202501 (2002)

Super-heavy elements – magic numbers

The nuclei around $^{254}_{102}\text{No}$ are deformed (\Rightarrow rotational bands)



Where is the next shell gap ?

model	Z	N
WS	114	184
FRDL	114	178
HFB	126	184
RMF	120	172

Synthesis of super-heavy elements gives direct information about their stability, but is extremely difficult:
 $\sigma = 4.5 \text{ pb}$ for $^{242}\text{Pu}(^{48}\text{Ca}, 4n)^{286}114$

Spectroscopy of nuclei around ^{254}No can give information about orbitals that originate from above the super-heavy shell closure.

odd nuclei probe
 single-particle structure

Prompt γ spectroscopy of ^{251}Md

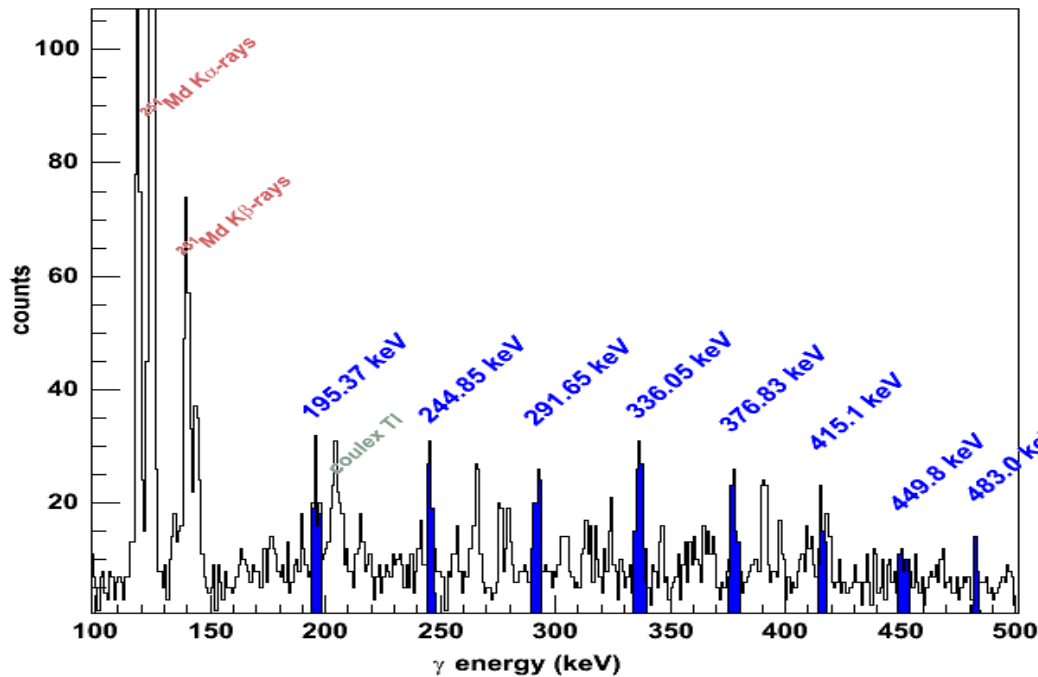
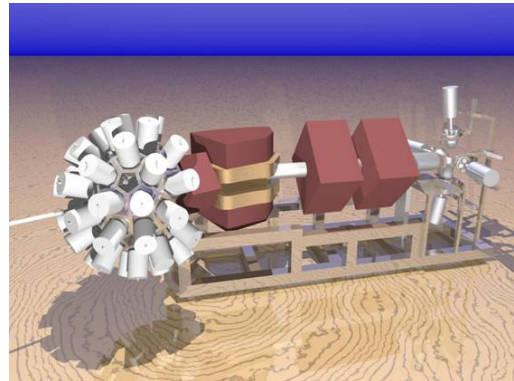
$^{205}\text{Tl}(^{48}\text{Ca}, 2n)^{251}\text{Md}$

$\sigma \sim 800 \text{ nb}$

2 weeks beam time

JUROGAM and RITU

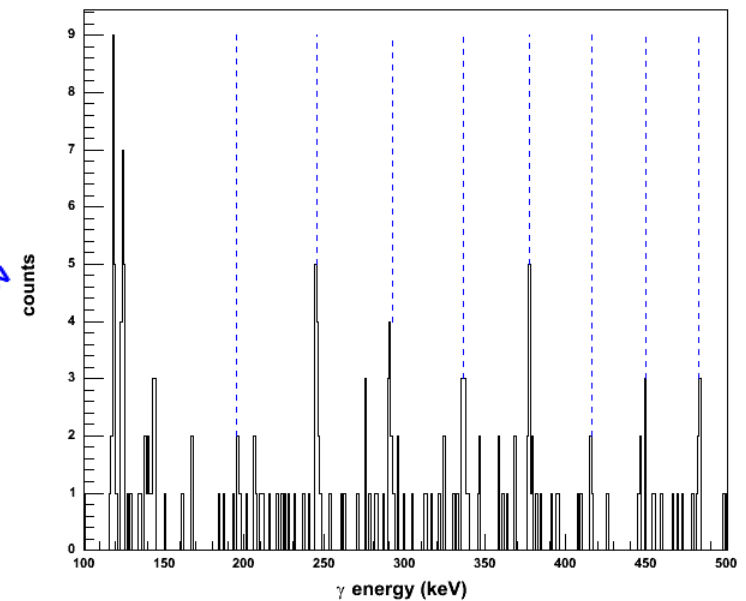
Jyväskylä



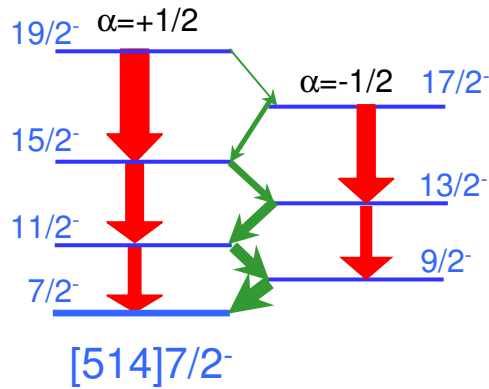
A. Chatillon et al., to be published

First rotational band in an odd nucleus with $Z > 100$

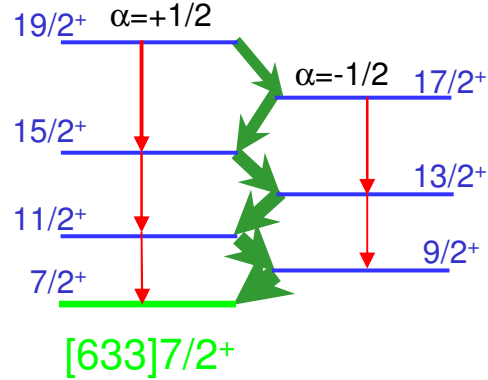
Gamma - Gamma coincidences



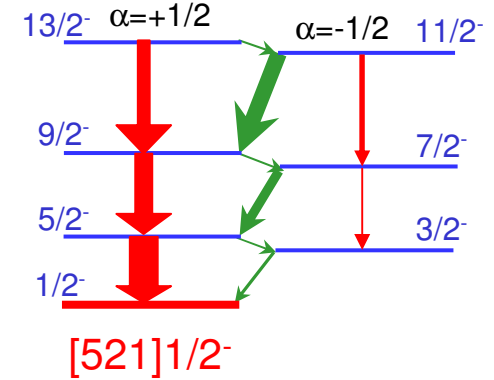
Electromagnetic properties of the rotational band in ^{251}Md



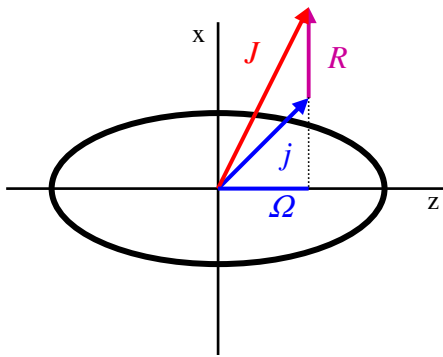
$g_K \sim 0.7 \Rightarrow$ mainly E2



$g_K \sim 1.3 \Rightarrow$ mainly M1



$g_K \sim -0.55, a \sim 1$
 \Rightarrow mainly one E2 band



Symmetries:

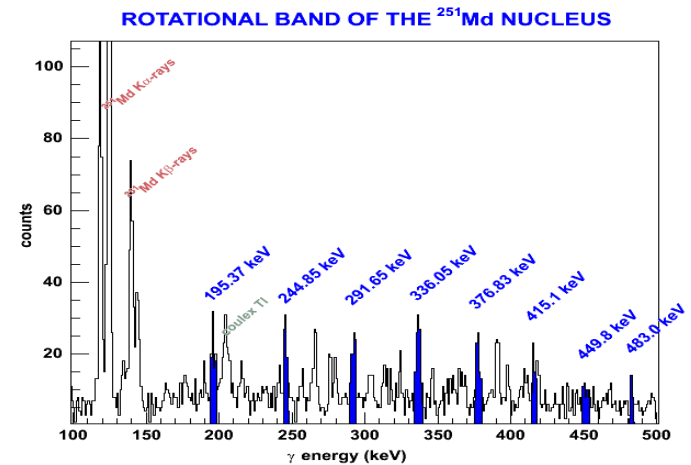
reflection $\hat{P} \Psi(\vec{r}) = \Psi(-\vec{r})$
 \Rightarrow parity eigenvalues ± 1

rotation $\mathcal{R}_x = e^{-i\pi J_x}$
 \Rightarrow signature $r_x = e^{-i\pi\alpha}$
 eigenvalues $r_x = \mp i, \alpha = \pm \frac{1}{2}$

$B(M1)/B(E2)$ depends on $(g_K - g_R)/Q_0$

for $K=1/2$ the Coriolis interaction
 decouples the two signatures:

$$E(I) = \frac{\hbar^2}{2\mathcal{J}} \left[I(I+1) - K^2 + a(-1)^{I+1/2} \left(I + \frac{1}{2} \right) \delta_{K,1/2} \right]$$

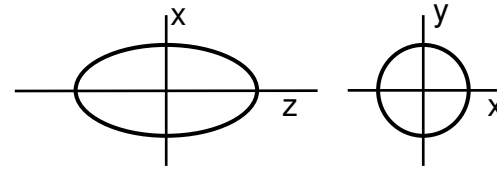


compatible with [521]1/2⁻ band

Quadrupole moments and transition rates

ellipsoid with symmetry axis z

electric quadrupole moment with respect to z



$$Q_0 = \frac{1}{e} \int (3z^2 - r^2) \rho(\vec{r}) d\tau = \frac{1}{e} \sqrt{\frac{16\pi}{5}} \int r^2 Y_{20}(\vartheta) \rho(\vec{r}) d\tau \quad \rho(\vec{r}) \text{ electric charge distribution}$$

intrinsic quadrupole moment in the body-fixed frame

$$\text{unit: } 1 \text{ b} = 10^{-28} \text{ m}^2 = 100 \text{ fm}^2$$

quadrupole moment and deformation parameter:

$$Q_0 = \frac{3}{\sqrt{5\pi}} Z R_0^2 \beta \left(1 + \frac{1}{8} \sqrt{\frac{5}{\pi}} \beta + \frac{5}{8\pi} \beta^2 + \dots \right) \quad R_0 = 1.25 A^{1/3} \text{ fm}$$

spectroscopic quadrupole moment observed in the laboratory frame

$$Q_s = \frac{3K^2 - I(I+1)}{(I+1)(2I+3)} Q_0 \quad (\text{we see immediately: } Q_s=0 \text{ for } I=0)$$

reduced transition probability

$$B(E2) = \frac{5}{16\pi} e^2 Q_0^2 \left| \langle I_i \ 2 \ K \ 0 | I_f \ K \rangle \right|^2$$

$$\text{unit: } 1 \text{ e}^2 \text{b}^2 = 10^4 \text{ e}^2 \text{ fm}^4$$

lifetime or transition rate

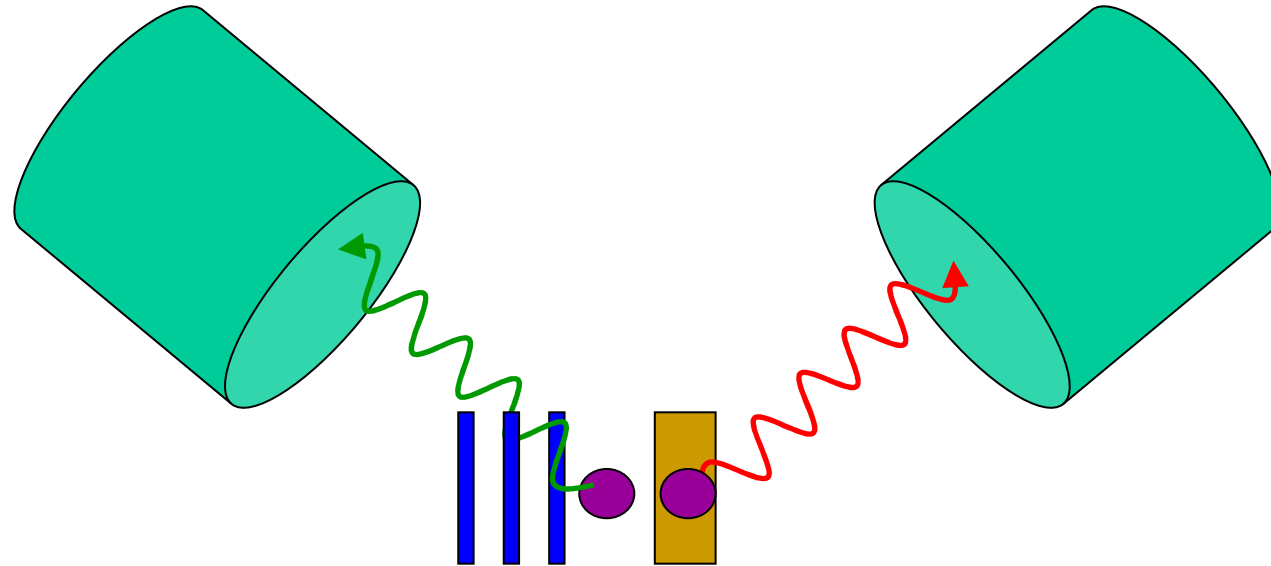
$$\lambda = \frac{1}{\tau} = 12.26 B(E2) E_\gamma^5 (1 + \alpha)$$

τ [ps], $B(E2)$ [$\text{e}^2 \text{b}^2$], E_γ [MeV],
 α conversion coefficient

Measuring lifetimes: Doppler shift methods

- Recoil-distance Doppler shift method: RDDS
 - 1 ps – 1 ns
 - Plunger with target and stopper or degrader foil
- Doppler-shift attenuation method: DSAM
 - 100 fs – 1 ps
 - backed target and lineshape analysis
- Fractional Doppler shifts: $F(\tau)$ method
 - 5 – 50 fs
 - thin target

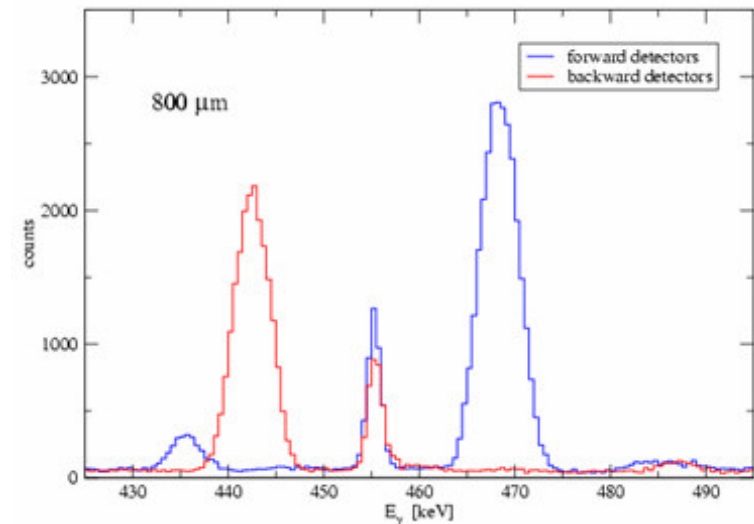
Recoil-Distance Doppler Shift Method



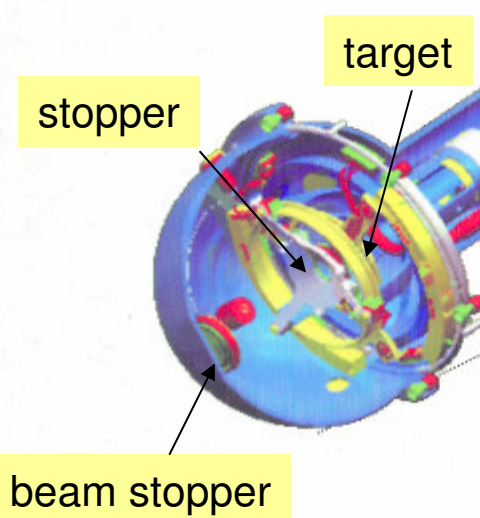
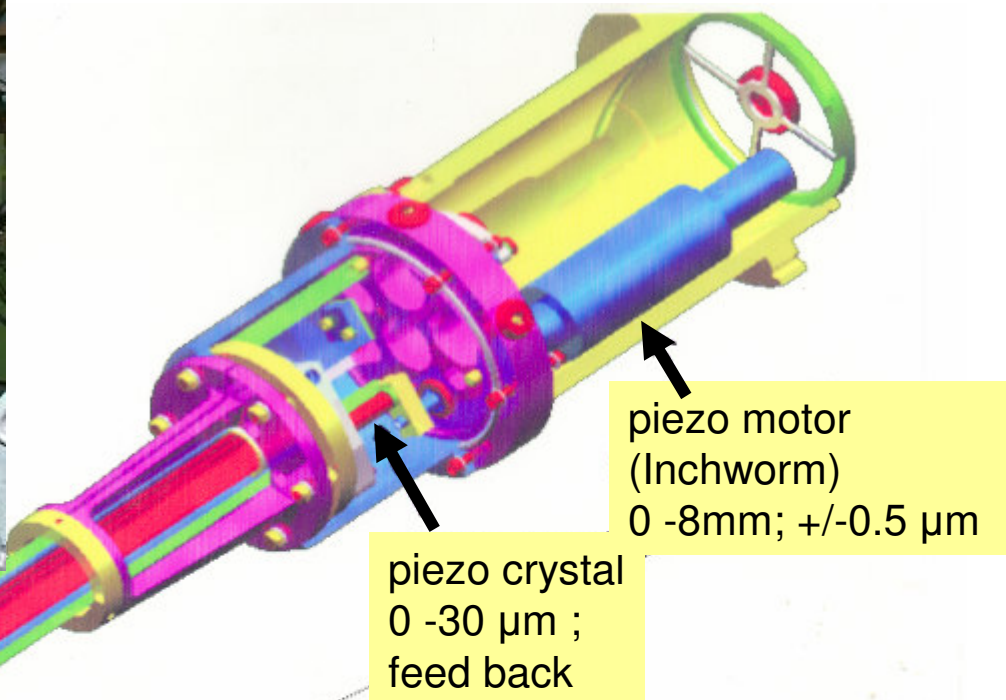
target and stopper foil at distance d
gamma rays are emitted

- in flight \Rightarrow peak Doppler shifted
- stopped \Rightarrow sharp peak at energy E_0

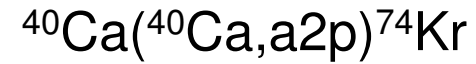
Lifetimes deduced from stopped and shifted intensities as a function of distance



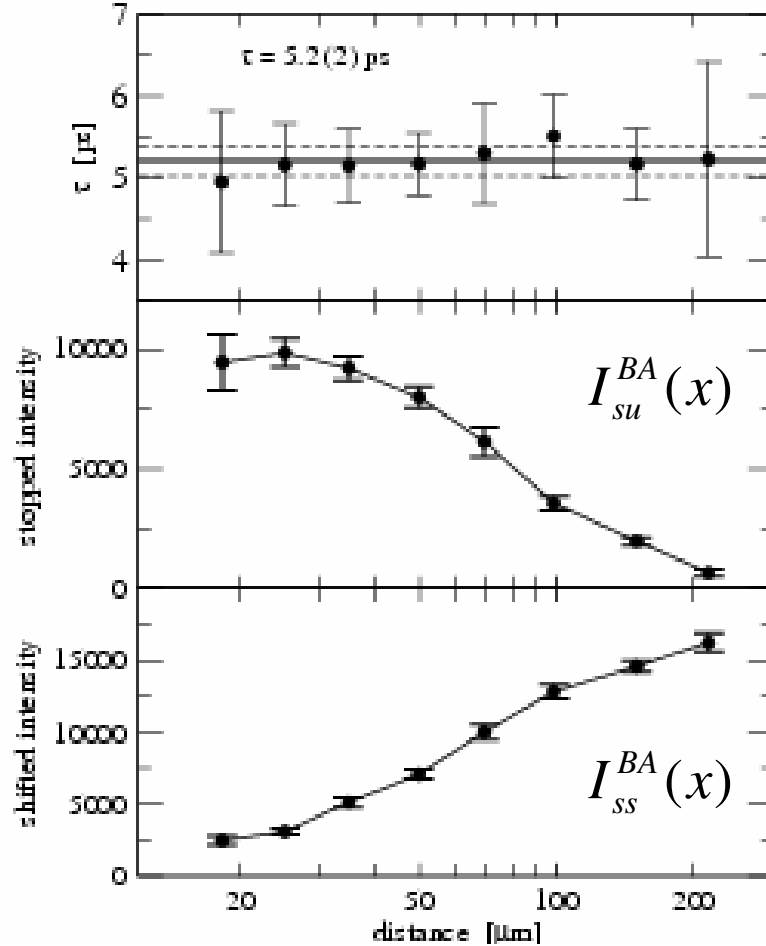
The Köln Plunger



Differential decay curve method

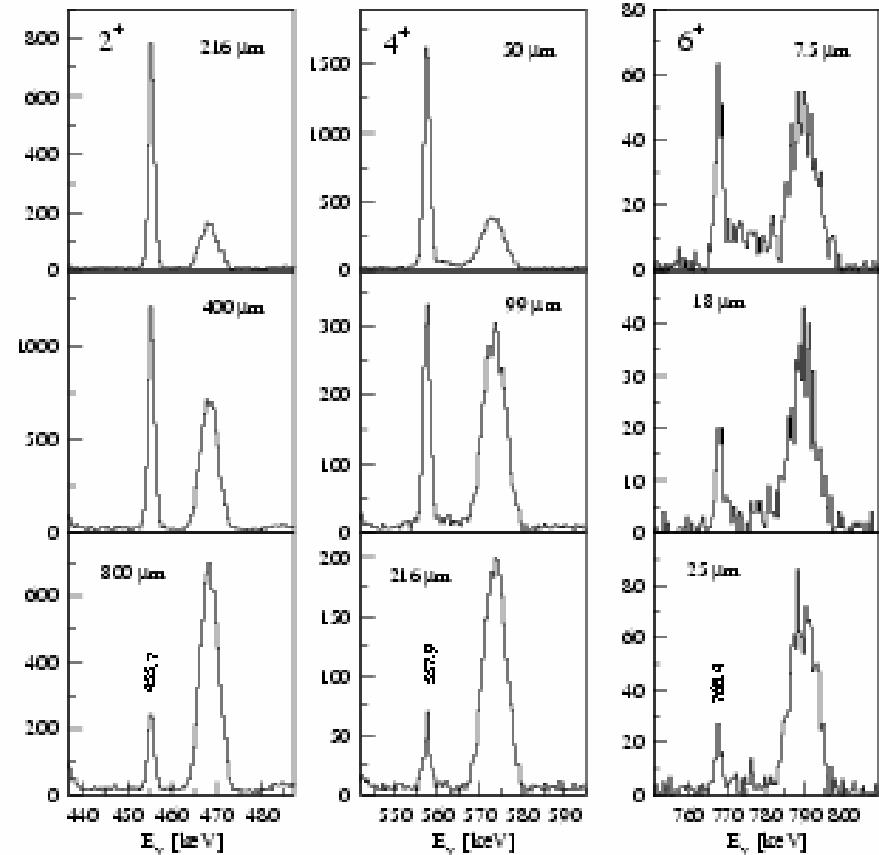


- forward detectors (36°)
- gated from above on shifted component

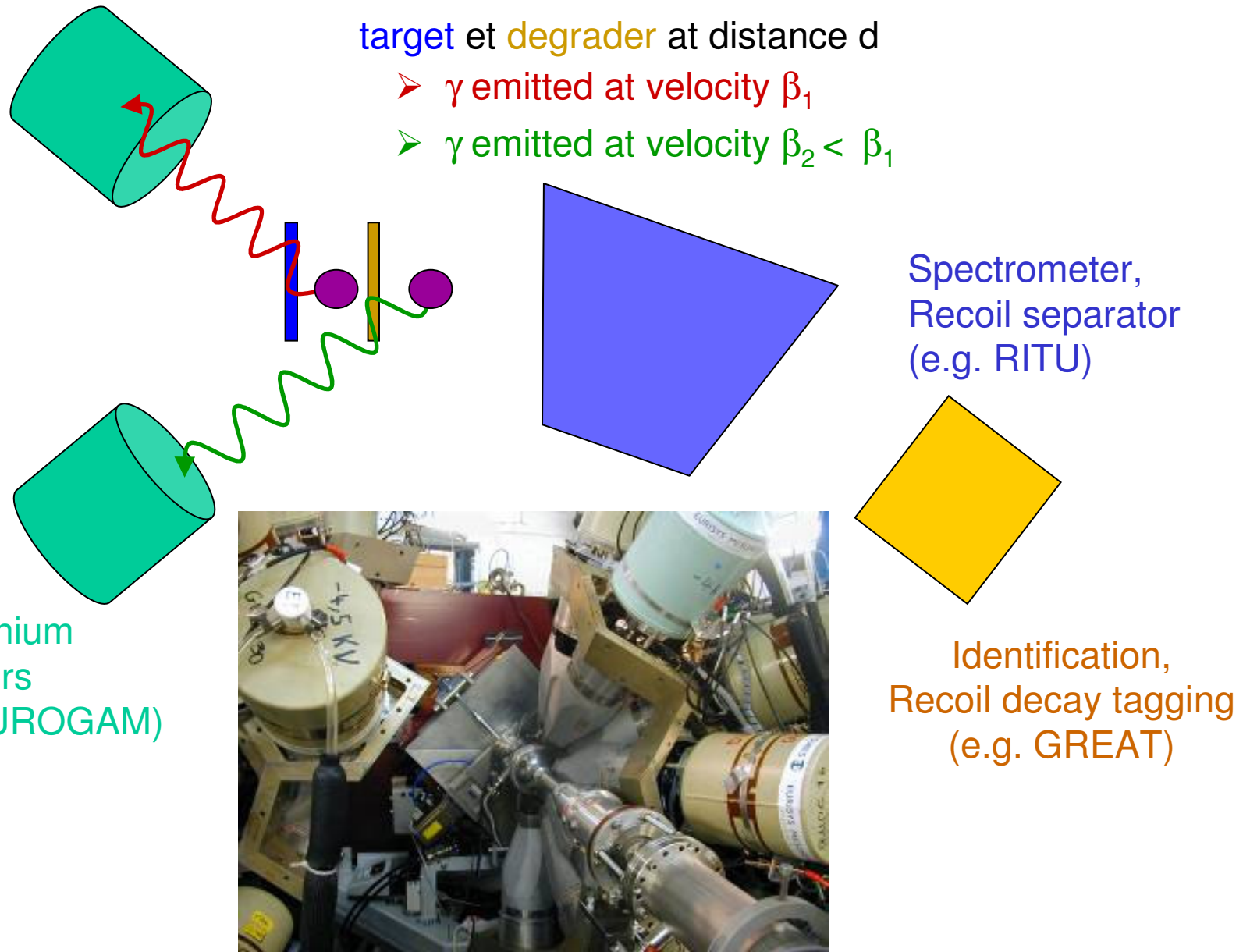


$$\tau = \frac{1}{\lambda_j} = \frac{I_{su}^{BA}(x)}{v \frac{d}{dx} I_{ss}^{BA}(x)}$$

A. Dewald et al., Z. Phys. A. 334, 163 (1989)



Differential Recoil-Distance Doppler Shift Method



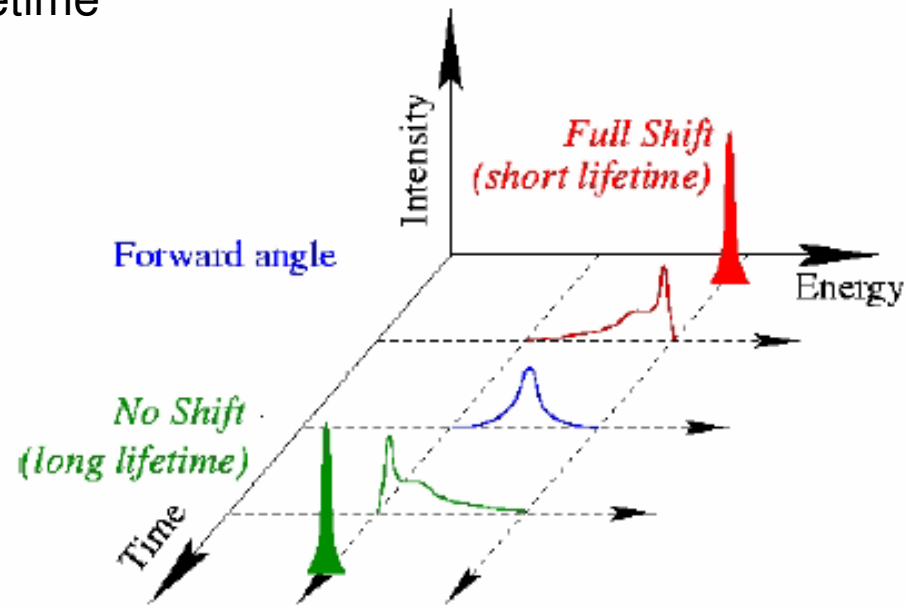
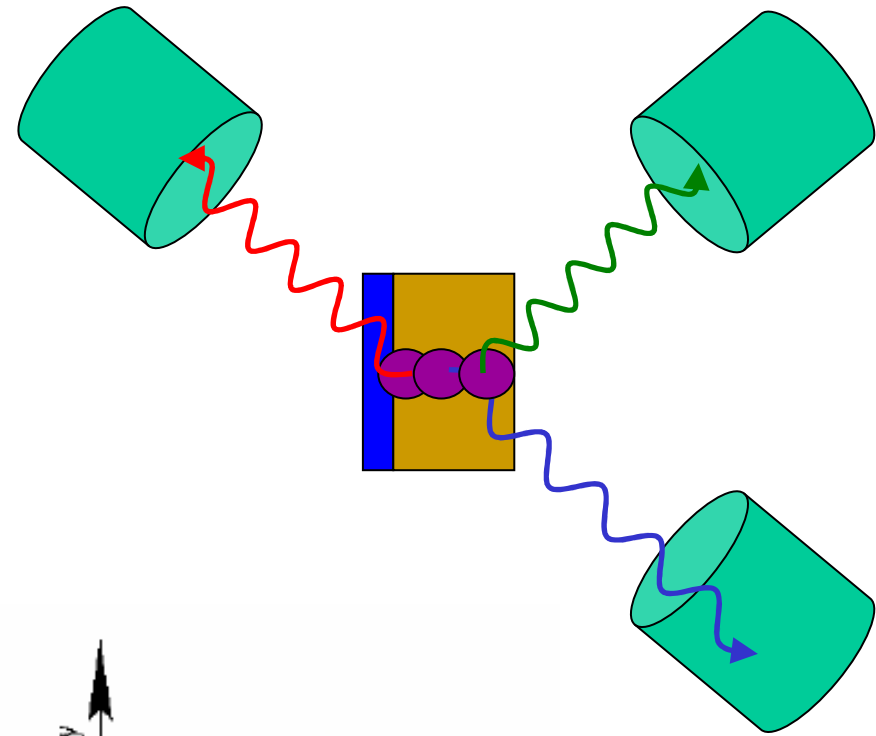
Doppler shift attenuation method

target with **backing**

gamma rays are emitted

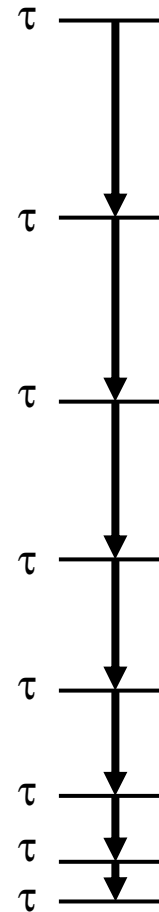
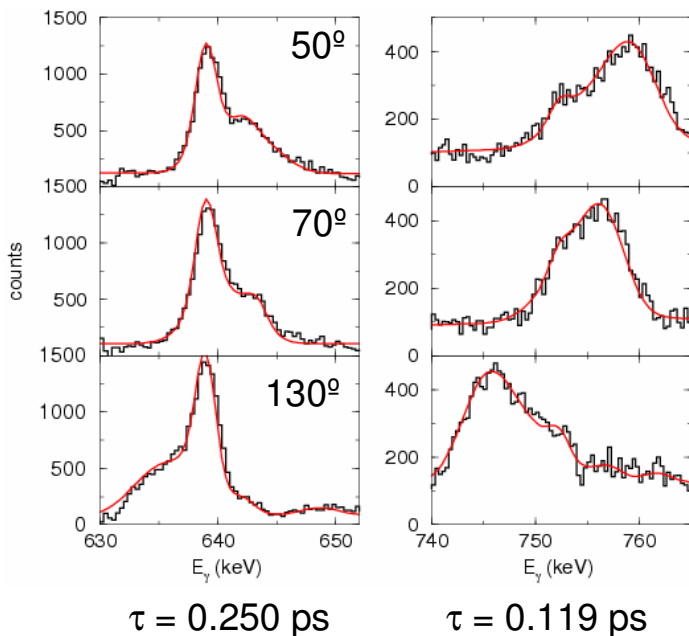
- with full recoil velocity
- slowed down
- finally stopped

Lineshape profile
characteristic for lifetime



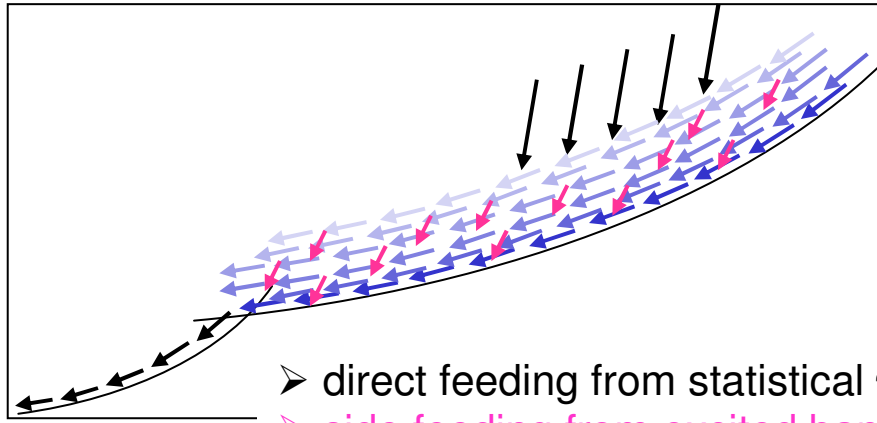
Lineshape analysis

- Simulate velocity history (3D) for recoils using Monte Carlo techniques based on reaction kinematics and stopping powers in target and backing
- convert velocity histories into line-shape profiles as seen by individual detectors (detector geometry and efficiency)
- compare simulated line shapes with observed peak profiles and minimize χ^2



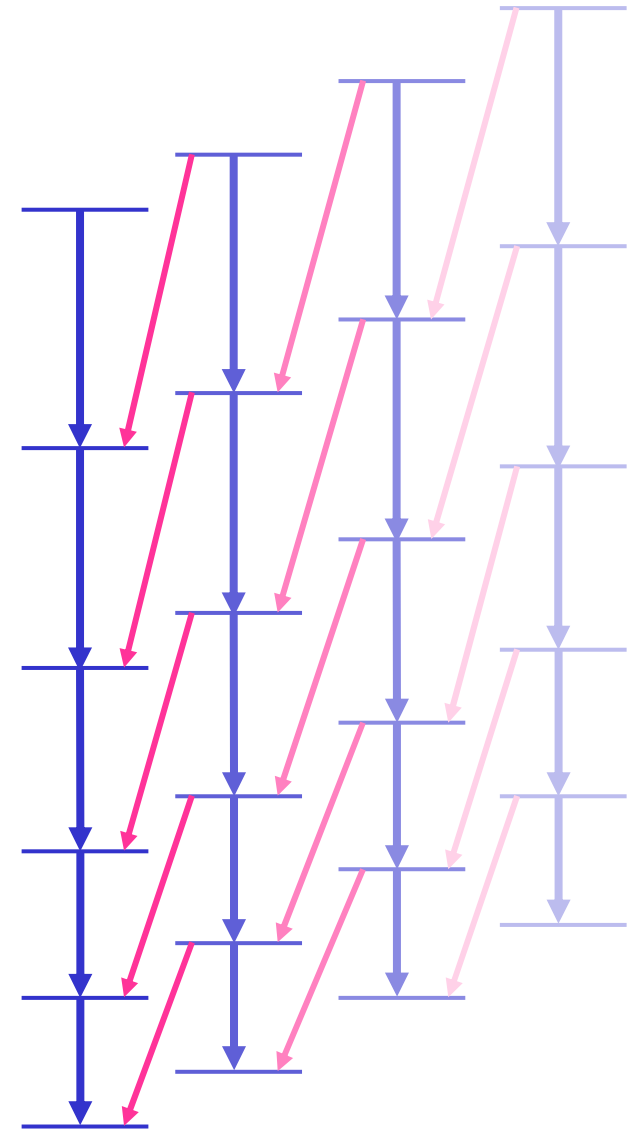
- Each state has its lifetime.
- We measure accumulated lifetime including those of all states above.
- We have to start at the top and work our way down.
- Once we have a first guess we can fit several transitions simultaneously.
- Finally we can fit all lifetimes of the entire cascade simultaneously.
- Side feeding is a problem.

Side feeding



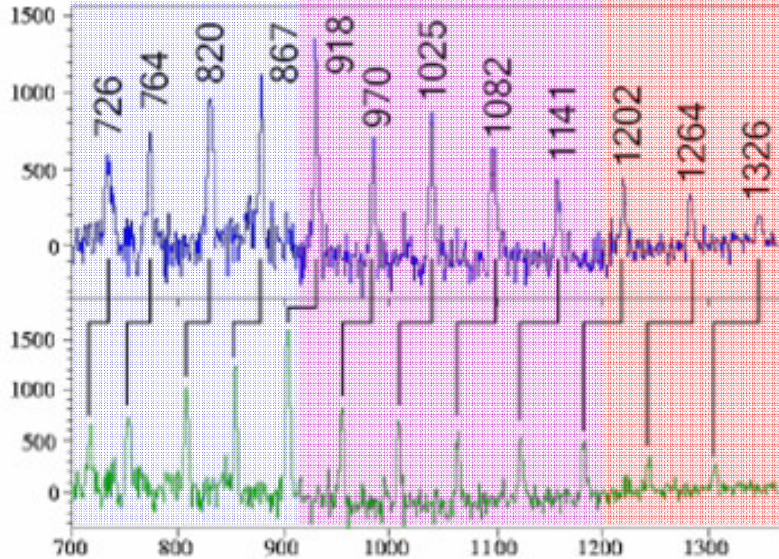
- direct feeding from statistical γ rays
- side feeding from excited bands
- in-band feeding

- It is impossible to measure all lifetimes of states above the one in question.
- We know the side-feeding intensity.
- Assume rotational model: side feeding comes from rotational band with fixed deformation (quadrupole moment).
- This allows to calculate feeding lifetime.
- Treat Q_{SF} as free parameter in the fit.
- Gating from above eliminates side feeding.

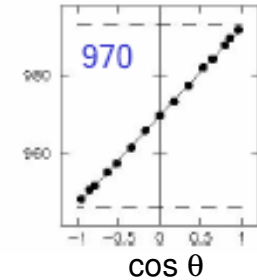
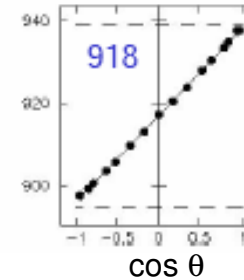
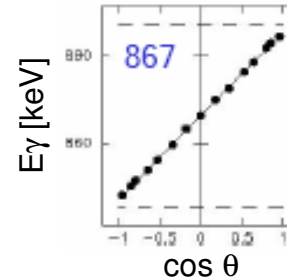


Fractional Doppler shifts – F(τ) method

thin target data



forward detectors (50°)
no Doppler correction



backward detectors (130°)
no Doppler correction

$$E_\gamma = E_0 \frac{\sqrt{1 - \beta^2}}{(1 - \beta \cos \vartheta)}$$

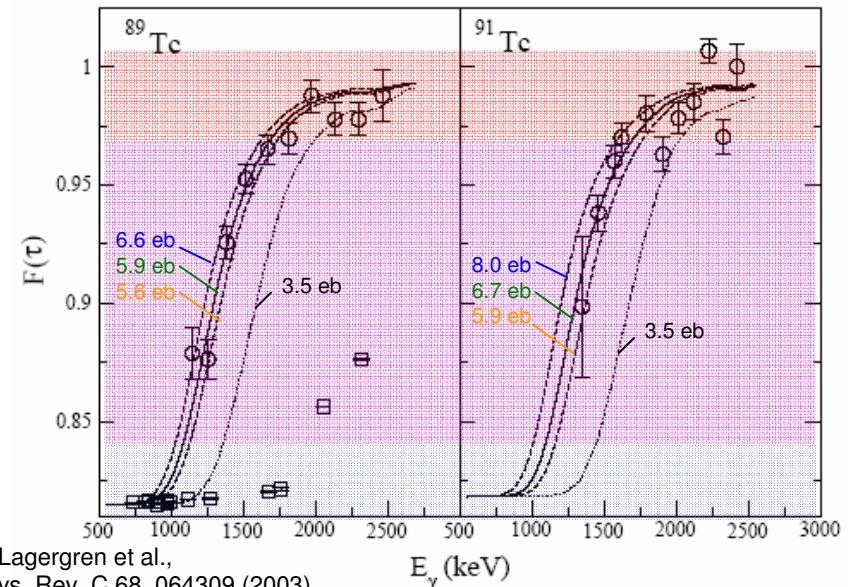
fit average recoil velocity
for each transition

very fast transitions at the top of the SD band
have almost the full initial recoil velocity: $F(\tau) \approx 1$

not quite as fast transitions are emitted still
within the thin target, but after the recoils have
been slightly slowed down, $F(\tau) \approx 0.9$

slower transitions at the bottom of the band and
ND transitions are emitted after the recoils have
left the target, $F(\tau) \approx 0.8$

- Extract quadrupole moment by comparing with simulation, including stopping powers.
- Gives quadrupole moment of the band, not individual lifetimes.



K. Lagergren et al.,
Phys. Rev. C 68, 064309 (2003)

$$F(\tau) = \frac{\beta}{\beta_0}$$

β average recoil velocity
 β_0 average initial recoil velocity

Magnetic moments

$$\vec{\mu}_I = g_K \mu_K \frac{\vec{I}}{\hbar}$$

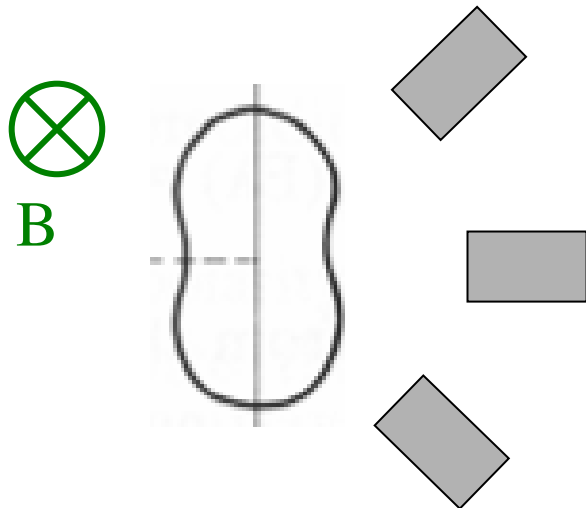
$$\mu_K = \frac{e\hbar}{2m_p c} = 3.152 \cdot 10^{-14} \frac{\text{MeV}}{\text{T}}$$

for a single nucleon with orbital angular momentum l and spin s : $\vec{\mu} = g_l \vec{l} + g_s \vec{s}$

for a proton $g_s=5.5858$ $g_l=1$
 for a neutron $g_s=-3.8261$ $g_l=0$

the resulting magnetic moment is very sensitive to the spins and their coupling, and therefore to the nuclear structure.

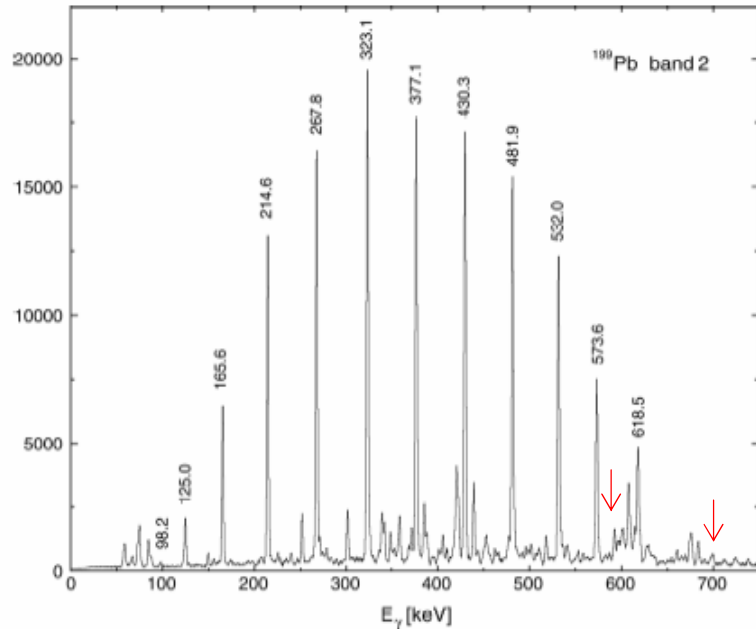
interaction with a magnetic field: $V_{\text{mag}} = -\vec{\mu} \cdot \vec{B} \Rightarrow$ Larmor precession



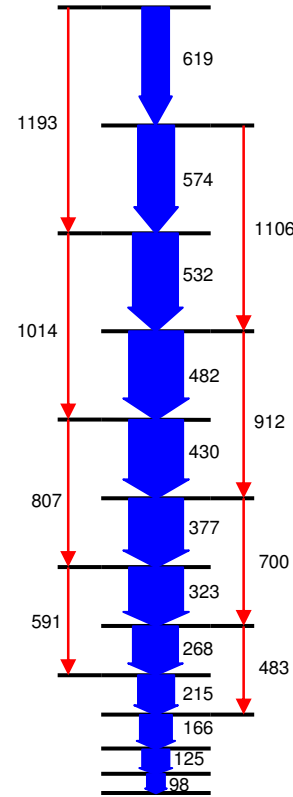
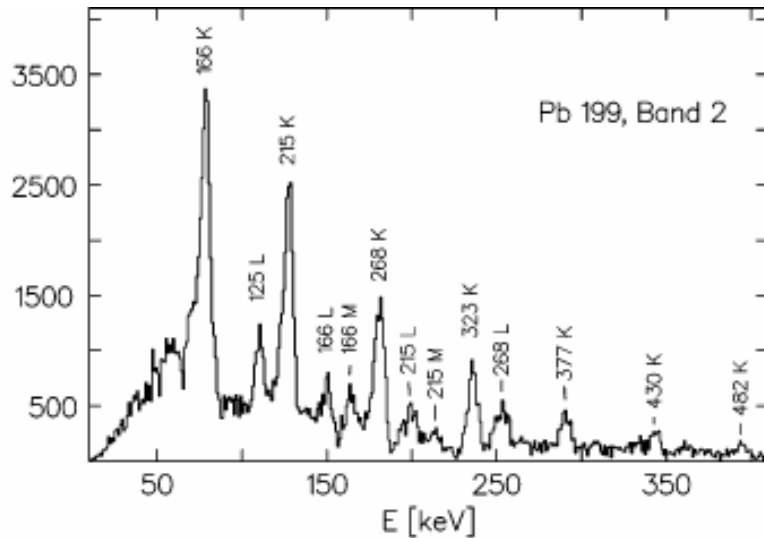
perturbed angular distribution

- apply magnetic field and measure angular distribution
- Larmor frequency gives g factor
- short lifetimes require strong fields
 - $\tau \sim \text{ns} \Rightarrow$ external field of a few Tesla
 - $\tau \sim \text{ps} \Rightarrow$ transient field ($\sim \text{kT}$) of ion passing through ferromagnetic medium (sandwich target)

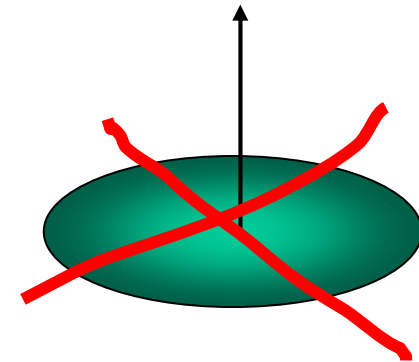
Rotational (?) bands in Pb isotopes



G. Baldisiefen et al., Phys. Lett. 275B, 252 (1992)



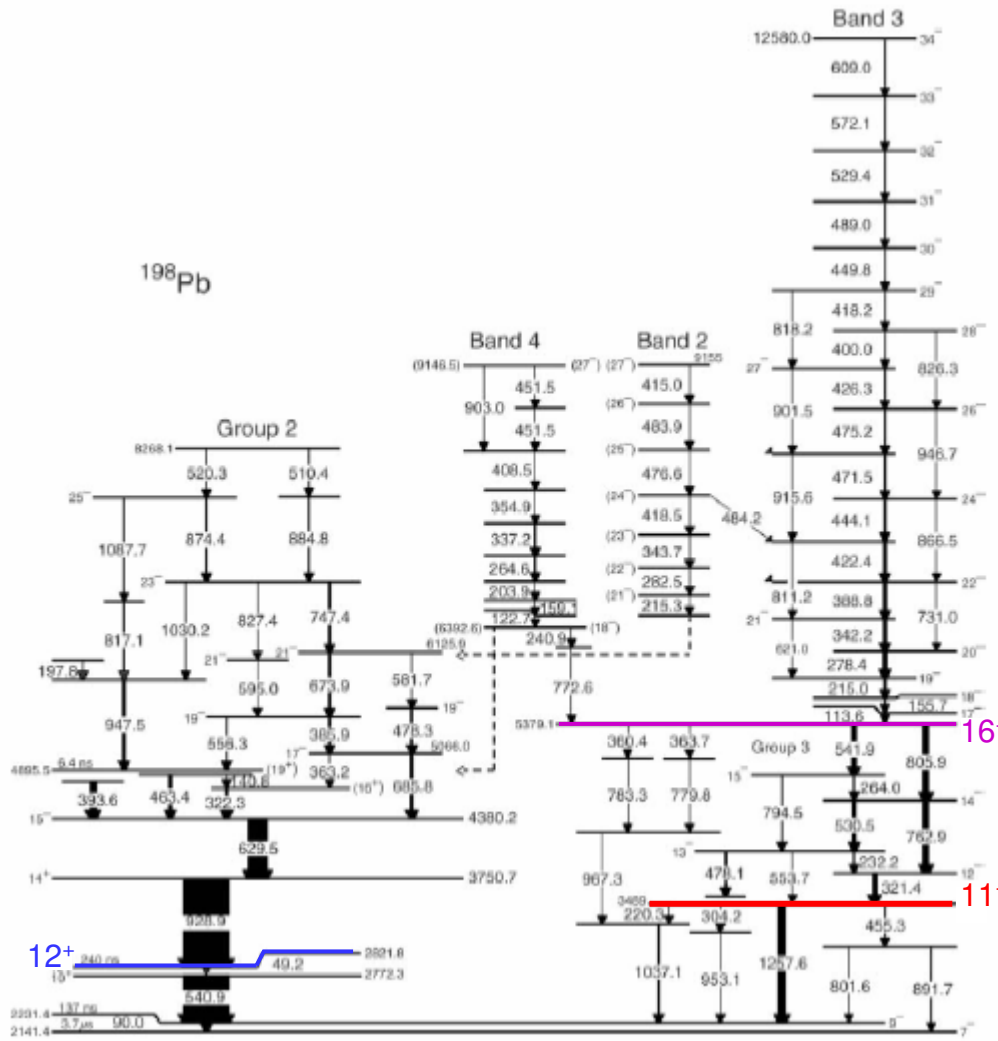
- Found throughout ^{191}Pb - ^{202}Pb and also in other mass regions.
- Very regular band of strong M1 transitions.
- The E2 transitions are very weak.
- This can't be a rotational band of a well-deformed nucleus.



Conversion-electron spectroscopy and linear polarization measurements confirm M1 character of the bands in Pb.

W. Pohler et al., Eur. Phys. J. A 5, 257 (1999)

Proton and neutron excitations in Pb

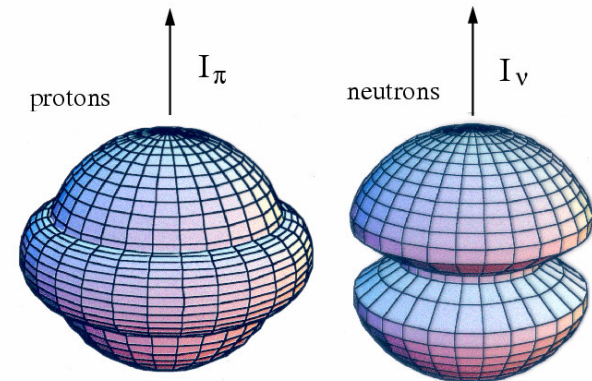


A. Gorgen et al., Nucl. Phys. A 683, 108 (2001)

closed proton shell
 proton excitations across the gap into the $\pi h_{9/2}$ or $\pi i_{13/2}$ shell possible
 e.g. $\pi(h_{9/2}i_{13/2})11^-$

open neutron shell
 neutron hole excitations in the $\nu i_{13/2}$ shell possible
 e.g. $\nu(i_{13/2}^{-2})12^+$

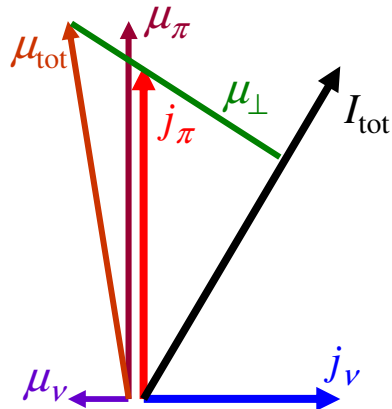
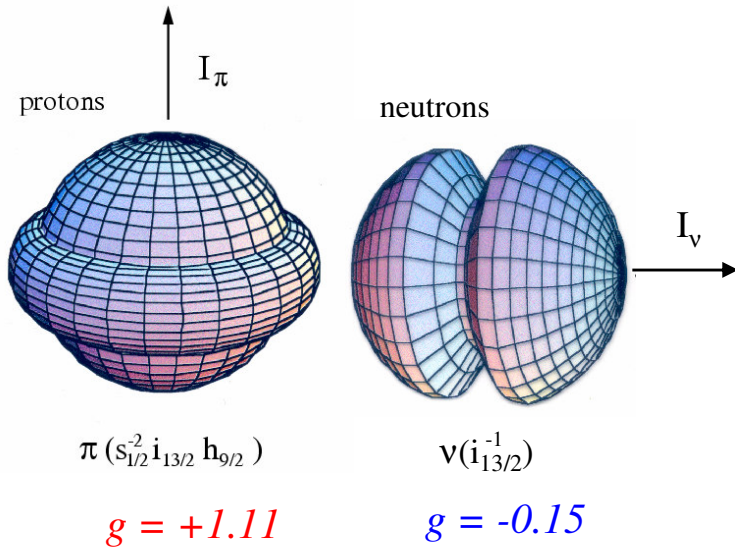
The M1 bands are not built directly on these states.
 Typical spin of the band head $\sim 16 \hbar$



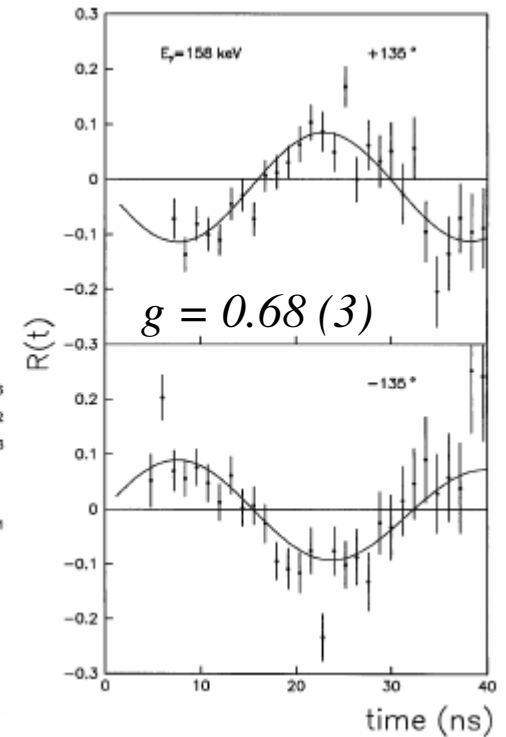
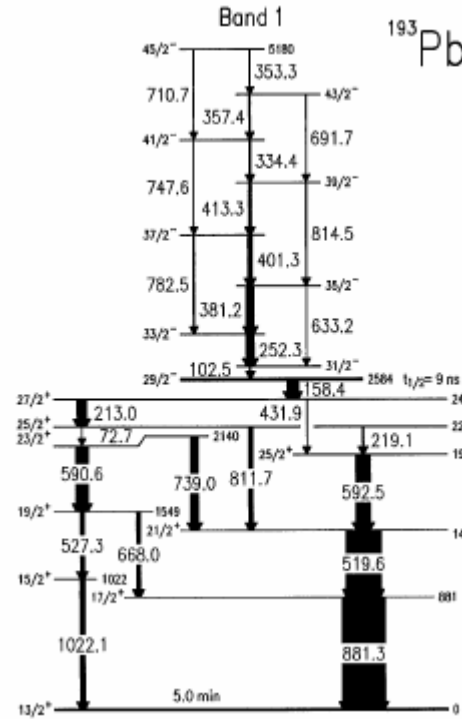
$$\pi (s_{1/2}^{-2} i_{13/2} h_{9/2})$$

$$\nu (i_{13/2}^{-1})$$

Magnetic Rotation

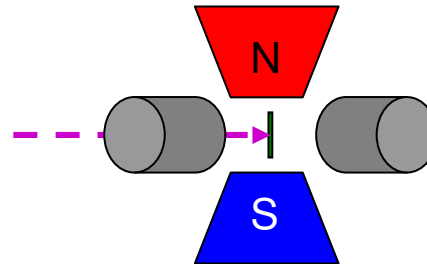


large transverse component of magnetic moment
 \Rightarrow generates strong M1 transitions



g factor measurement for band head in ^{193}Pb :
 time-differential perturbed angular distribution (TDPAD)

$^{170}\text{Er}(^{28}\text{Si}, 5n)^{193}\text{Pb}$
 pulsed beam
 (1.3ns/400ns)



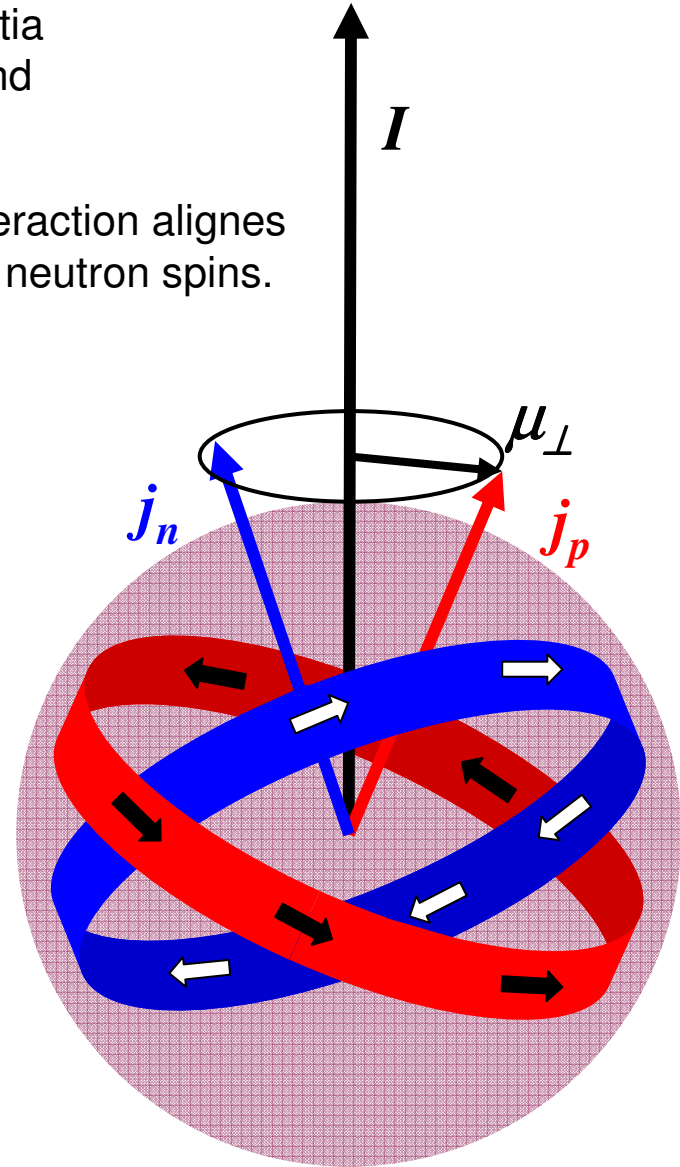
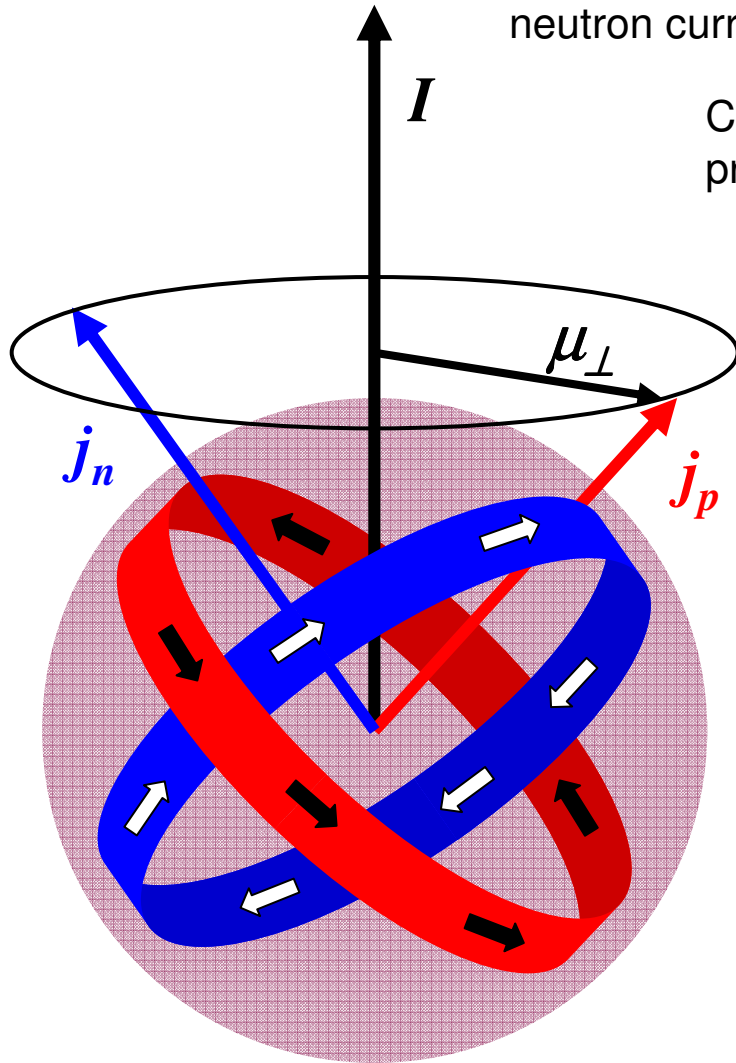
Shell-model classification	g factor ^b
$\nu i_{13/2}^{-1} \otimes \pi (h_{9/2} i_{13/2})_{11}$	0.713(16) ^c
$\nu (i_{13/2}^{-2})_{12} f_{5/2}$	-0.070(05)
$\nu (i_{13/2}^{-2})_{12} f_{5/2} \otimes \pi (s_{1/2} i_{13/2})_7$	0.112(10)
$\nu (i_{13/2}^{-2})_{12} f_{5/2} \otimes \pi (h_{9/2}^2)_8$	0.088(07)
$\nu (i_{13/2}^{-2})_{12} f_{5/2} \otimes \pi (i_{13/2}^2)_{12}$	0.385(15)
$\nu (i_{13/2}^{-1} f_{5/2}^2)_{21/2} \otimes \pi (s_{1/2} h_{9/2})_5$	0.361(07)

S. Chmel et al., Phys. Rev. Lett. 79, 2002 (1997)

Shears effect

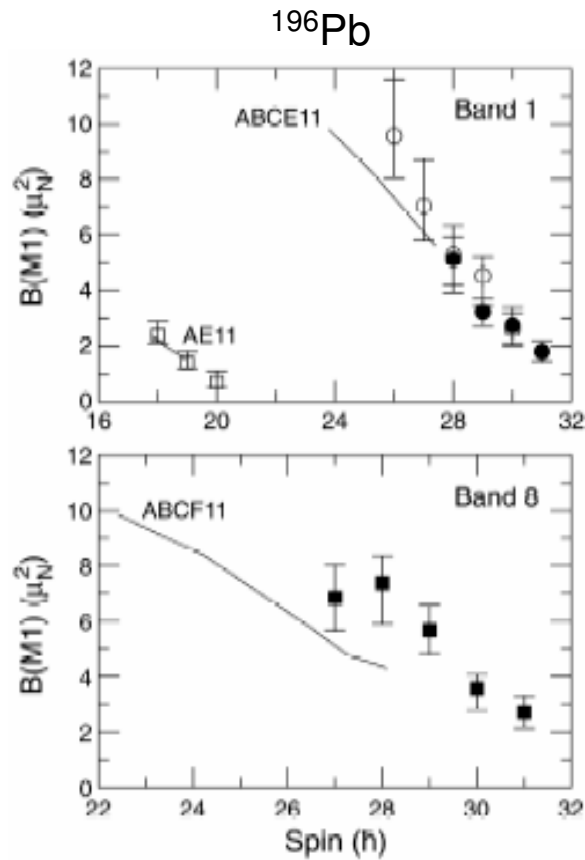
Large moment of inertia comes from proton and neutron currents.

Coriolis interaction aligns proton and neutron spins.



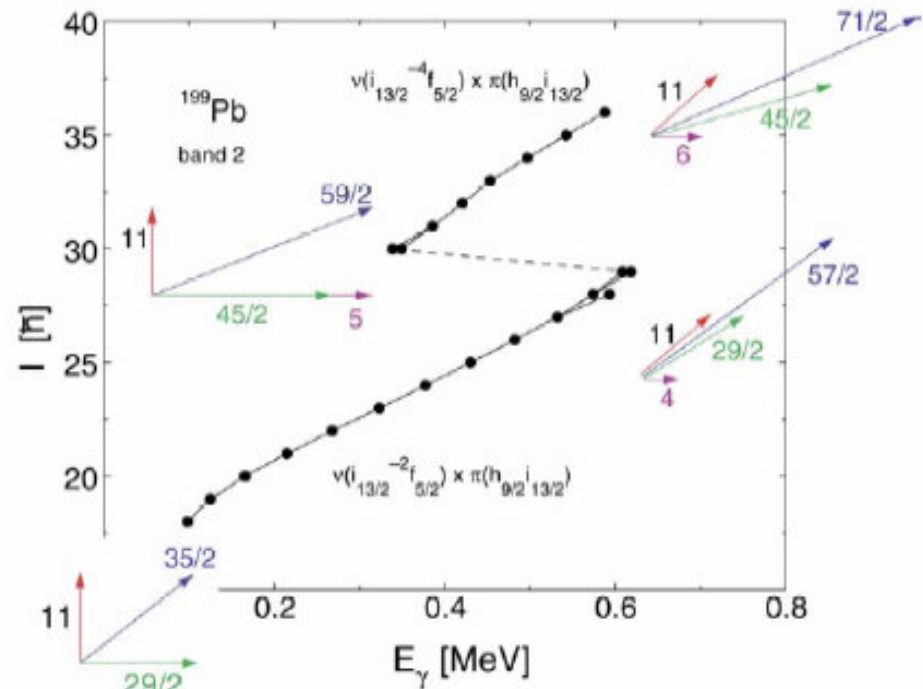
S. Frauendorf, Nucl. Phys. A 557, 259 (1993)

Shears effect



R.M. Clark et al., Phys. Lett. B 440, 251 (1998)
 A.K. Singh et al., Phys. Rev. C 66, 064314 (2002)

- Lifetime measurements (DSAM and RDDS) confirm characteristic decrease of $B(M1)$ values.
- Good agreement with Tilted Axis Cranking (TAC) calculations.



- When the shears are closed, more angular momentum can be generated by breaking a pair (of neutrons) and the (bigger) shears open again.